A computer approach to finding an optimal log landing location and analyzing influencing factors for ground-based timber harvesting

Marco Contreras and Woodam Chung

Abstract: Locating a log landing is an important task in forest operations planning. Several methods have been developed to find an optimal landing location and compute a mean skidding distance, but they simplify harvest unit attributes and do not simultaneously consider multiple design factors influencing optimal landing locations. In this study, we introduce a computerized model developed to determine the optimal landing location for ground-based timber harvesting. Using raster-based GIS data, the model finds skid trails from stump to each of candidate landings and selects the best landing location that minimizes total skidding and spur road costs. The model is applied to several hypothetical harvest units with different terrain and harvest volume attributes to analyze the effects of design factors influencing optimal landing locations. Unit boundary shapes, volume distribution, the presence of obstacles, terrain conditions, and spur road construction are considered as influencing design factors.

Résumé : Le choix de l'emplacement d'une jetée est une tâche de planification importante en opérations forestières. Plusieurs méthodes ont été développées afin de trouver l'emplacement optimal des jetées et de calculer la distance moyenne de débardage. Par contre, toutes ces méthodes tendent à simplifier les attributs de la parcelle de récolte et ne permettent pas de tenir compte simultanément des nombreux facteurs qui influencent l'emplacement optimal des jetées. Dans cette étude, nous présentons un modèle informatique conçu pour déterminer l'emplacement optimal des jetées pour des opérations de débardage sur le terrain. Utilisant les données de type matriciel d'un SIG, le modèle localise les sentiers de débardage de la souche jusqu'à chacune des jetées envisagées et sélectionne le meilleur emplacement, c'est-à-dire celui qui permet de minimiser le coût total de débardage et de construction des routes forestières de desserte. Le modèle est appliqué à plusieurs parcelles hypothétiques de récolte ayant des conditions de terrain et de volume différentes afin d'analyser les effets des facteurs qui influencent l'emplacement optimal des jetées. La forme du contour des parcelles, la distribution du volume, la présence d'obstacles, la condition du terrain et la construction de chemin de desserte sont considérées comme des facteurs qui influencent l'emplacement optimal des jetées.

[Traduit par la Rédaction]

Introduction

Locating a log landing for a given harvest unit is a frequent and important task in forest operations planning because landing locations largely affect not only logging costs but also environmental impacts such as site disturbances. In addition to harvesting and road costs, several factors related to forest characteristics and terrain conditions are usually considered when landing locations are selected. These factors may include timber volume distribution, irregular harvest unit boundaries, terrain conditions, and the presence of obstacles that may change skidding directions. A variety of numerical procedures and computer models have been developed to identify optimal landing locations and compute mean skidding distances (MSD). However, most of them simplify harvest unit attributes and do not simultaneously consider multiple design factors that may influence optimal landing locations.

Research related to the economic consideration in forest operations has its origin in the beginning of the 20th century. According to Greulich (2003), Bradner et al. (1933) presented calculations of an MSD to a continuous landing, and the calculation of MSD for circular cable settings with a central landing was introduced by Brandstrom (1933) as approximately two thirds of the external skidding distance. The book *Cost control in the logging industry* (Matthews 1942) presents the first widely accepted numerical procedure to estimate an MSD. Based on the centroid and equal area arguments, Matthews developed formulas to calculate an MSD for a harvest unit with uniform volume in a regularly shaped boundary, such as squares, rectangles, wedges, and circles. An improvement of the Matthews procedure was later made by Suddarth and Herrick (1964). Based on the integral formula $\text{MSD} = \int x dA/A$, where x is the distance from a log landing to a log pickup point and A is the area to be harvested, they developed mathematical equations for more accurate calculations of an MSD for the same regular geometric shapes. Furthermore, a mathematical equation for any kind of triangle was established (Peters 1978), and sev-

Received 5 May 2006. Accepted 10 August 2006. Published on the NRC Research Press Web site at cjfr.nrc.ca on 20 April 2007.

M. Contreras and W. Chung.[1] Department of Forest Management, College of Forestry and Conservation, University of MT, Missoula, MT 59812, U.S.A.

[1]Corresponding author (e-mail: woodam.chung@umontana.edu).

 doi:10.1139/X06-219

eral models were developed to calculate optimal road and landing spacing on unbounded tracts (Matthews 1942; Peters 1978; Thompson 1992; Liu and Corcoran 1993).

Irregular shapes of a unit's boundary and nonuniform volume distribution were included in numerical procedures developed in 1970s. Peters and Burke (1972) established a method to calculate an MSD on irregularly shaped areas. A procedure that incorporates variable log density on irregular shapes was later built by Donnelly (1978). In addition, Perkins and Lynn (1979) developed a method that directly incorporates the roughness of the terrain into the MSD calculation. The Perkins and Lynn method also addresses the case where straight skidding is not feasible. These approaches use coordinate data to calculate an MSD, where the data are taken from topographic maps. More recent approaches use polygonal mesh approximations to represent the harvest area (Greulich 1989). A model that uses a digital elevation model (DEM) to calculate skidding distance and MSD was also developed (Tucek 1999). Although this method presents a more realistic calculation of the skidding distance by calculating accumulated slope lengths from cell to cell, the 50 m resolution used may not be able to accurately describe terrain conditions.

Using these previous methods to calculate an MSD and other mathematical theories of optimization, several algorithms and models were developed to find the optimal location of a centralized landing. Love (1972) developed an optimization algorithm to identify an optimal location of a facility for rectangular areas by minimizing a total cost function through derivatives. Greulich (1991) developed an optimization algorithm that can be applied to any polygonal region and considers unevenly distributed volume by introducing harvest area partitions. However, those algorithms do not take into account uneven terrain, the presence of skidding obstacles, or activity-confining concave-shaped unit boundaries.

Two main objectives of this study are (*i*) to develop a computerized model to find the optimal location of a centralized log landing that simultaneously considers skidding cost, access road cost, irregularly shaped unit boundaries, terrain conditions, uneven timber volume distribution, and the presence of skidding obstacles and (*ii*) to analyze the effects of the above factors on the optimal log landing location using hypothetical harvest units under different terrain and volume attributes. Skidding obstacles are introduced in this study as a design factor that may influence landing locations. When skidding across unit boundaries is not allowed because of different ownerships or riparian zones, the boundary often becomes an obstacle that changes skid trails. Small steep areas within a harvest unit where skidders cannot negotiate also become obstacles for skidding. The presence of these obstacles forces the shortest skid trails to be rerouted, which results in the increase of skidding distances. In this paper, we present the computerized model developed and the effects of these influencing factors on the optimal landing location.

Computerized model

A harvest unit is defined in this paper as an area to be harvested by ground-based timber harvesting systems where all logs will be brought into a single centralized log landing. Harvest units are usually delineated by forest engineers or field managers while considering forest characteristics, terrain conditions, stream locations, and existing road networks among others. It is assumed that a log landing can be located anywhere within the harvest unit and will be accessed by a spur road. In this context, finding an optimal landing location becomes a cost-minimization problem that considers skidding, spur road construction and hauling costs to be incurred to harvest the entire unit.

The computerized model we developed uses a complete enumeration method to solve the cost-minimization problem. Even though many combinatorial optimization problems have been solved using more intelligent solution techniques (Roberts 1984), we used the complete enumeration because (*i*) it guarantees the solution optimality under the given data resolution, and (*ii*) a harvest unit constitutes a relatively small-scale problem that is solvable in a reasonable amount of time.

A DEM representing a harvest unit is the main input data of the model along with a volume layer. A volume layer for the model can be created from a polygon-based stand volume map by transforming it into a raster that has the same resolution as the DEM. Every single grid cell in a DEM becomes a candidate log landing location in the model. When the model evaluates a candidate landing all the other grid cells containing timber volume are assumed to be log pickup points. Using the complete enumeration method, the model first calculates the total harvesting cost (THC) associated with each of candidate landing locations and it then selects the least cost landing location as the optimal centralized landing location within the harvest unit:

$$[1] \qquad \mathrm{THC}_k = \mathrm{TSC}_k + \mathrm{RC}_k$$

where TSC_k is the total skidding cost associated with candidate landing location k and RC_k represents the road construction and hauling cost along the spur road that connects the candidate landing to the existing road network through the least-cost path. In the case that the spur road is to be used temporarily, the spur road construction cost may also include road decommissioning cost.

Estimating total skidding cost

The model calculates TSC by adding up all the skidding costs from each grid cell to the candidate landing location:

$$[2] \qquad \mathrm{TSC}_k = \sum_{i=1}^{m} \mathrm{SC}_i$$

where m represents the total number of grid cells within the harvest unit and SC_i represents the skidding cost from the ith grid cell on the harvest unit to grid cell k which represents the landing location. The skidding cost is calculated using the following equation:

$$[3] \qquad \mathrm{SC}_i = \left[\left(\frac{\mathrm{CT}_i}{60}\right) \times \mathrm{RR}\right] \times \mathrm{NT}_i$$

where CT_i is a skidding cycle time in minutes for a round trip between landing and log pick up point, RR represents the rental rate of a skidder expressed in US dollars per hour, and NT_i indicates the number of turns necessary for skidding all timber volume on the ith grid cell to the landing. For the applications presented in this paper, we used US$85/h for the skidder rental rates and assumed the timber volume per turn (payload capacity) was 1.5 m^3. Cycle times can be estimated using appropriate regression models. As an example, we used the following equations in the applications to estimate downhill and uphill skidding cycle times, respectively, after modifying a regression model introduced by Han and Renzie (2005):

[4] $$CT_{ds} = 3.9537 + 0.0215D_i$$

[5] $$CT_{us} = 3.9537 + 0.0258D_i$$

where CT_{ds} is the cycle time for downhill skidding, CT_{us} is the cycle time for uphill skidding, and D_i is the skidding distance along the slope from the ith grid cell to the landing location. The downhill cycle time equation was also used to predict the cycle time on flat ground in our applications.

Distance from cell i to cell k is calculated by adding the slope distance of adjacent grid cells located along a straight line joining the two cells (Fig. 1). The solid line in Fig. 1 shows the direct distance along the slope from the log landing location (the grid cell with a circle) to a log pick-up point. The shaded line shows how the actual distance along the slope is calculated in the model, going from the centroid of a grid cell to the centroid of the adjacent cell on the black line's course. When cells i and k are on the same column or the same row, or they are located perfectly diagonal, both solid and shaded line distances are equal. Otherwise, the slope distance calculated by the model is greater than the direct slope distance between the two cells. Because the distance calculated by the model follows a winding course instead of a straight line, the wander factor commonly used by other methods (Segebaden von 1964; Peters and Burke 1972; Donnelly 1978; Greulich 1991) is omitted in this model.

The presence of obstacles that may change skidding directions is taken into consideration when the distance along the slope is calculated. One case of these obstacles would be a harvest unit boundary in a concave shape where skidding across the boundary is not allowed because of different ownerships or natural boundaries, such as streams (Fig. 2*a*). Another case would be small and narrow steep area that skidders cannot negotiate and have to go around to reach the other side of the area (Fig. 2*b*). Besides these two cases, any other zones where heavy machinery traffic should be limited, such as wetlands and unstable soils, can be specified as obstacles and entered into the model. When an obstacle is encountered between the landing and log pick up point, the model identifies grid cells representing boundaries of the obstacle and selects the shortest path that connects the landing to the log pick up point without invading the obstacle boundary grid cells (Fig. 2).

Once the model calculates the total skidding costs associated with each of candidate landings (all the grid cells within the harvest unit), it selects one grid cell with the minimum total skidding cost. This grid cell represents the optimal log landing location without considering spur road construction.

Estimating total road cost

The total road cost (TRC) associated with the ith grid cell is defined as the cost of building a spur road that connects the ith grid cell to an existing road (or any of user-defined timber exit point) at a minimum construction plus hauling cost along the spur road. To determine the least cost road location, the model builds a road network consisting of a set of nodes and links. Nodes represent grid cells, and links represent the connections to the adjacent nodes (Fig. 3). In the model, each node is connected to the eight adjacent nodes. Figure 4 illustrates an example of a road network representing a harvest unit.

Fig. 1. Distance calculation along the slope in the model.

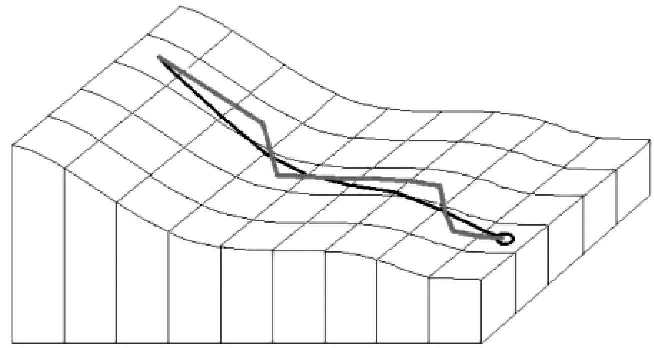

After a road network is built, the model estimates a spur road construction cost per link using the following equation:

[6] $$RCC_{link} = D_{link} \times URCC \times TF$$

where RCC_{link} is the road construction cost of a link, D_{link} is the horizontal distance of the link in metres, URCC is a constant unit cost of road construction (US dollars per horizontal metre along the centreline), based on a relatively flat terrain, and TF is total factor, which is a multiplier that increases road construction costs caused by steep terrains. The TF is calculated using the following equation:

[7] $$TF = SF \times SSF$$

where SF is slope factor and SSF is side slope factor. These user-defined multipliers are determined by the link's road gradient and side slope, respectively. Side slope is calculated based on the elevation difference and horizontal distance between two side cells of the front cell of a link (shaded line in Fig. 5). Road gradient is calculated based on the elevation difference of two cells forming a road link (solid line in Fig. 5).

As an example, Table 1 shows link gradient and side slope ranges along with their corresponding SF and SSF values. These values were used in the applications described in this paper.

After RCC_{link} is calculated for each link, a road network problem is formed to find the least cost spur road location from a given candidate landing to the existing road. RCC_{link} is used as the link attribute value, and the objective function is to minimize total RCC_{link}. The model uses the Dijkstra's shortest path algorithm (Dijkstra 1959) to find the least cost spur road location and estimate the road construction cost from each of the candidate landings to the existing road. The shortest path algorithm used in the model is known to be efficient and has been widely used to determine the

Fig. 2. Skidding distance calculation along the slope where obstacles exist. The shaded line shows the skidding distance estimated by the model.

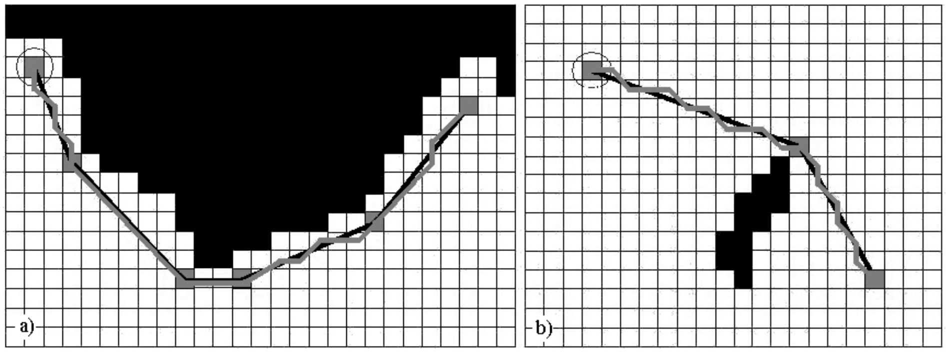

Fig. 3. Links connecting a cell with its eight adjacent cells.

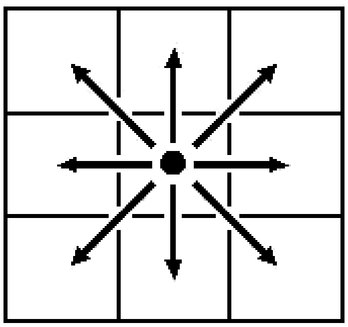

Fig. 4. A road network created by the model for a given harvest unit. The shaded cell represents the takeoff point from an existing road.

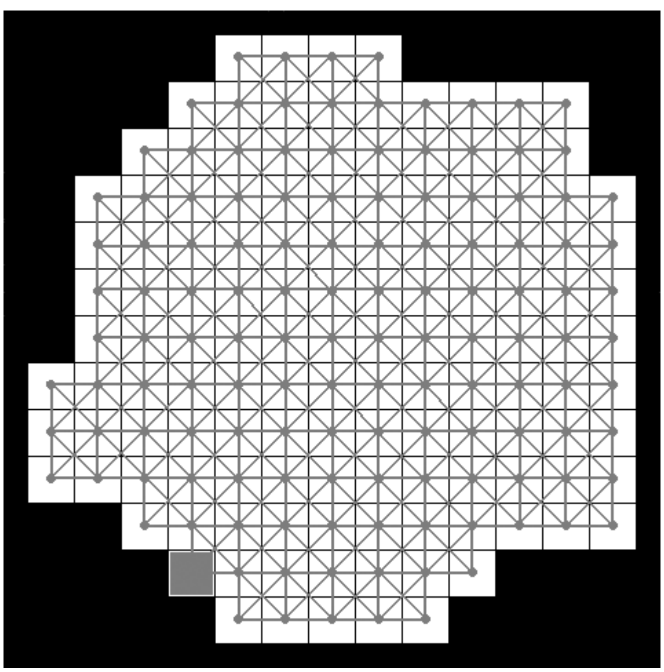

shortest path between two points in a given road network (Tan 1999; Chung et al. 2004; Anderson and Nelson 2004).

Once the least cost spur road location is found from each of candidate landings (all the grid cells in the harvest unit) to the existing road, the associated length of the spur road is calculated to determine the hauling cost over the spur road. Considering a log truck rental rate of US$60/h and a mean truck speed of 10 km/h, the hauling cost per truck per metre on the spur road is US$0.006/m. Assuming log trucks have a maximum load capacity of 20 m^3, hauling cost (HC) over a spur road is calculated using

$$[8] \qquad HC = \left(\frac{V_t}{20}\right) 0.006 D_{road}$$

where V_t is the total volume (m^3) in the harvest unit and D_{road} is the horizontal distance of the spur road in metres. HC is then added to the spur road construction cost to calculate the total road cost (TRC) for a given candidate landing to the existing road. This additional increase of TRC may affect the optimal landing location by shortening spur road length depending on trade-offs between TRC and TSC.

Fig. 5. Grid cells used to calculate the side slope and road gradient of a given road link.

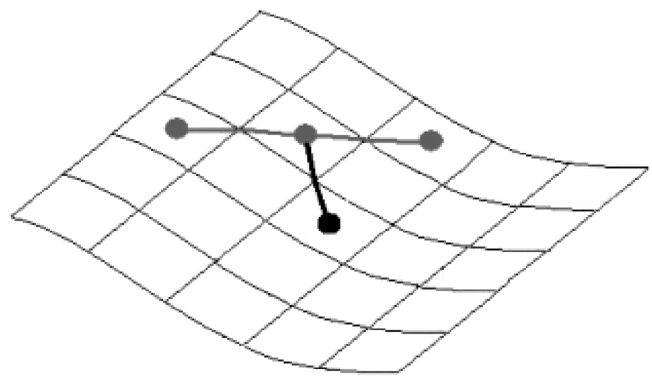

Table 1. Road gradient and side slope factors used to increase road construction cost in steep terrains.

Range of road gradient	Corresponding link's slope factor	Range of side slope	Corresponding link's side slope factor
0.00–0.05	1.0	0.00–0.15	1.0
0.06–0.10	1.5	0.16–0.30	1.5
0.11–0.15	2.5	0.31–0.45	2.5
0.16–0.20	3.5	0.46–0.60	3.5
0.21–0.25	5.0	0.61–0.75	5.0
0.26–0.30	6.0	0.76–0.90	6.0
>0.30	10.0	>0.90	10.0

Table 2. Test polygons for optimal landing location comparisons.

Rectangle	Scalene triangle	Convex polygon

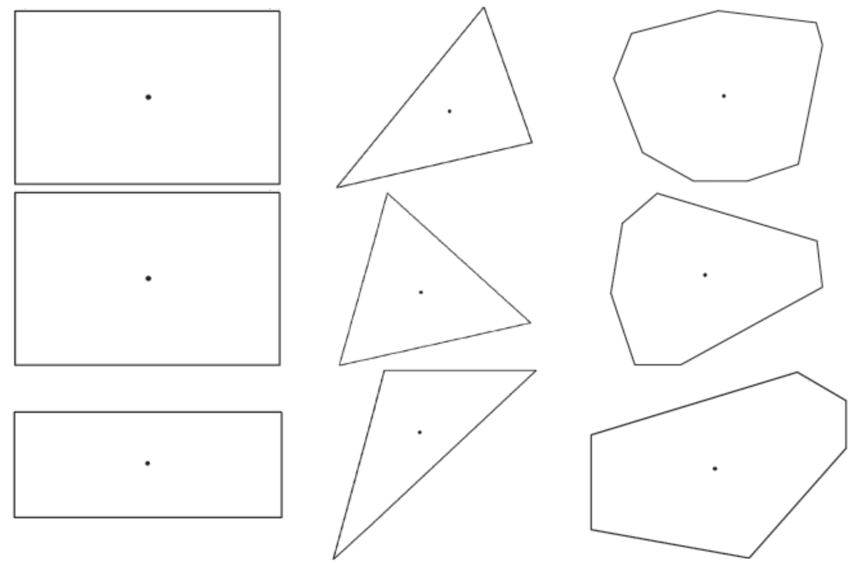

Table 3. Comparisons of the model results with Greulich (1991) in the optimal landing locations.

Shape and coordinates	Optimal landing location coordinates (*x*,*y*)			Difference	
	Greulich 1991	Model 1[a,c]	Model 2[b,c]	Greulich – model 1	Greulich – model 2
Rectangles					
Point 1 (0,0), point 2 (600,0), point 3 (600,400), point 4 (0,400)	(300,200)	(305,195)	(300.5,199.5)	7.07	0.71
Point 1 (0,0), point 2 (360,0), point 3 (360 240), point 4 (0,240)	(180,120)	(185,115)	(180.5,119.5)	7.07	0.71
Point 1 (0,0), point 2 (160,0), point 3 (160,60), point 4 (0,60)	(80,30)	(85,25)	(80.5,29.5)	7.07	0.71
Scalene triangle					
Point 1 (0,0), point 2 (400,100), point 3 (300,400)	(238.84,167.47)	(235,165)	(238.5,167.5)	6.34	0.34
Point 1 (0,0), point 2 (400,100), point 3 (100,400)	(166.44,166.44)	(165,165)	(166.5,166.5)	2.03	0.08
Point 1 (0,0), point 2 (400,400), point 3 (100,400)	(166.48,274.14)	(165,275)	(166.5,274.5)	1.71	0.36
Irregular shapes					
Point 1 (10,250), point 2 (40,330), point 3 (190,370), point 4 (360,350), point 5 (370,310), point 6 (330,100), point 7 (240,70), point 8 (150,70), point 9 (60,120)	(196.20,224.16)	(195,225)	(196.5,224.5)	1.46	0.45
Point 1 (50,70), point 2 (10,190), point 3 (30,310), point 4 (90,360), point 5 (360,280), point 6 (370,200), point 7 (130,70)	(164.27,216.31)	(165,215)	(164.5,216.5)	1.50	0.30
Point 1 (10,150), point 2 (10,290), point 3 (310,380), point 4 (380,340), point 5 (380,270), point 6 (240,110)	(193.24,241.56)	(195,245)	(193.5,241.5)	3.86	0.27

[a]Optimal landing location using a DEM resolution of 10 m × 10 m.
[b]Optimal landing location using a DEM resolution of 1 m × 1 m.
[c]The *x* and *y* coordinates are represented by the centre of the grid cell selected as the optimal landing location.

Model verification

Instead of using mathematically derived formulas, our model uses a complete enumeration method, which allows us to examine individual skidding patterns and consider various terrain and volume attributes. To verify the results of our model, MSD comparisons were made with the model developed by Greulich (1991), which has been verified as being accurate in his paper. We developed nine hypothetical harvest units (polygons) on uniform, flat terrain with evenly distributed volume. These units include three rectangles, three scalene triangles, and three irregular shaped convex polygons of different sizes (Table 2). Both models were applied to these polygons to identify optimal landing locations based only on skidding costs that are linear with distance. All polygon boundaries represented by *x* and *y* coordinates of multiple vertices were directly entered into the Greulich's model (Table 3); each polygon had to be converted into a raster for our model. We used ArcGIS Spatial Analyst tool to convert polygons to raster in two different grid resolutions (10 m × 10 m and 1 m × 1 m). Optimal landing locations found by both models are compared in Table 3.

Whereas the Greulich model identifies the optimal landing location as a point, our model selects a grid cell. Unlike a point, a grid cell is an area that can be represented by any point within the area. We used the centre of the grid cell to present its location in Table 3. The results shown in Table 3, due to this reason, appear to show that there are differences between the two models. The differences are, however, solely caused by raster data representation of harvest units required for our model. The landing locations found by the Greulich model are located within or at least on the border of the grid cells selected by our model, which indicates that the two models found the same optimal landing locations. Data specificity decreases and errors can be introduced when spatial data are converted from a vector to a raster (Clarke 2003). The fact that the differences decrease when a smaller grid cell size is used (Table 3) confirms that the raster data representation of harvest units is the source of the differences between the two models.

We also tested our model against widely known mathematical equations derived to estimate MSD in a given geometry of harvest unit. MSD was computed for all the polygons mentioned above from the optimal landing location selected by our model with a 10 m × 10 m resolution (Table 3, model 1). We used the mathematical formula presented by Suddarth and Herrick (1964) to estimate MSD for the rectangles. For the scalene triangles, the MSD formula developed by Peters (1978) was used. In the irregularly shaped polygon cases, the polygons were divided into triangles, and then Peters' formula was applied to each triangle. The MSD was then calculated as an area-weighted mean. Both equations are presented in Table 4. The MSDs calculated by our model, which uses the complete enumeration method based on a grid representation of the polygons, are compared with the results of the formulas (Table 5). These results show marginal differences between the formulas and the model. The fact that the differences are within one grid cell confirms again that the raster representation of harvest unit is the cause of the differences.

Applications

Hypothetical harvest units

Three hypothetical harvest units[2] were developed to analyze the effects of irregularly shaped harvest units, timber volume distribution, sloped terrain, the presence of obstacles, and different spur road costs on the optimal log landing location (Fig. 6). All the units have the same size (20.9 ha), and a 10 m × 10 m DEM was developed for each unit. Harvest unit 1 represents a regularly shaped unit (Fig. 6*a*), whereas units 2 and 3 represent irregularly shaped harvest units (Figs. 6*b* and 6*c*).

We ran the model on these hypothetical harvest units to find optimal landing locations under 16 sets of different terrain and timber volume attributes. Cases 1–3 are based on harvest units 1–3, respectively, and used to evaluate the effects of the boundary shape on the optimal landing location. These cases are examined under flat terrain, a uniform timber volume distribution of 300 m^3/ha (3.0 m^3 per grid cell), and no obstacles of any kind. The effect of obstacles caused by a concave-shaped harvest unit boundary (Fig. 2*a*) is analyzed in cases 4 and 5, which are based on harvest units 2 and 3, respectively. To evaluate the effect of terrain conditions, cases 6, 7, and 8 were developed using harvest unit 1 with a maximum slope inclination of 20%, 30%, and 40%, respectively (Fig. 7). The effect of obstacles caused by steep areas that skidders cannot pass through (Fig. 2*b*) are analyzed in cases 9, 10, and 11, which present one, two, and four obstacles, respectively (Fig. 8). These cases are also based on harvest unit 1 with a maximum slope inclination of 30%. Obstacle areas (small steep areas) were created within the unit with a mean slope of 80%. The effect of timber volume distribution is evaluated in harvest unit 3 with different volume distributions. Case 12 has two volume zones of the same size with different volume distributions: 150 m^3/ha and 300 m^3/ha, making an overall mean volume of 225 m^3/ha (Fig. 9*a*). Case 13 has three different volume zones: 150 m^3/ha, 300 m^3/ha, and 450 m^3/ha with an overall mean volume of 300 m^3/ha (Fig. 9*b*). To evaluate the effect of different spur road construction and hauling costs on the optimal landing location, cases 14–16 were developed. Cases 14, 15, and 16 consider a spur road construction cost of US$10/m, $20/m, and $30/m, respectively. Based on harvest unit 1, these cases are examined under uniform volume distribution of 300 m^3/ha, no obstacles of any kind and a maximum slope inclination of 30% on uneven terrain. The solid grid cell in Fig. 10 illustrates the location where the spur road is to be taken off from the existing roads. Table 6 summarizes the terrain and timber volume conditions for the 16 different cases.

Actual harvest unit

Although hypothetical cases 1–16 are used to describe how each of the individual terrain and volume attributes influences the optimal landing location, we also applied the model to an actual harvest unit in a realistic setting. The harvest unit is located in the Mica Creek watershed, the Potlatch's Experimental Forest in northern Idaho. It is assumed that the harvest unit is designed to be clear-cut, and a centralized log landing is constructed within the unit along with a spur road that connects the landing with the existing road located along the bottom of the hill (Fig. 11). The selected harvest unit for the case study is 11.8 ha in size with a mean volume of 450 m^3/ha. Some areas within the harvest unit that have >40% slope are considered to be obstacles for skidding activities (solid grid cells in Fig. 12).

Results and discussion

The computer model was run for each of the cases described in the previous section to identify the optimal centralized log landing location. The landing locations are indicated by a single solid cell along with its row and column numbers in Figs. 13–22. Estimated THC associated

[2] Harvest unit data can be downloaded from http://www.cfc.umt.edu/chung/publications.

Table 4. MSD (=ASD, average skidding distance) formulas developed for rectangles and scalene triangles.

Presented by Suddarth and Herrick (1964)

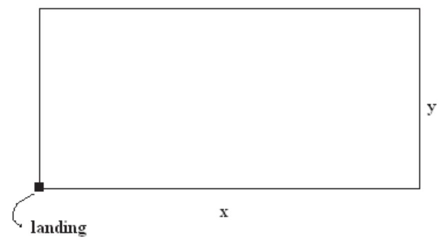

$$\mathrm{ASD}=\frac{\sqrt{x^2+y^2}}{3}-\left(\left[\frac{y^2}{6x}\right]\ln\left[\tan\left\{\frac{\arctan\left(\frac{y}{x}\right)}{2}\right\}\right]\right)-\left(\left[\frac{x^2}{6y}\right]\ln\left[\tan\left\{\frac{\arctan\left(\frac{x}{y}\right)}{2}\right\}\right]\right)$$

Developed by Peters (1978)

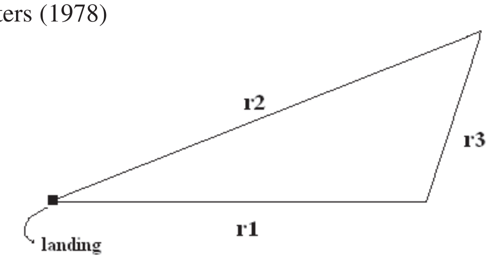

$$\mathrm{ASD}=\left(\frac{r1+r2}{6r3^2}\right)\left[r3^2+(r1-r2)^2\right]+\left(\left[\frac{\{r3^2-(r1-r2)^2\}\{(r1+r2)^2-r3^2\}}{12r3^3}\right]\ln\left[\frac{r1+r2+r3}{r1+r2-r3}\right]\right)$$

Table 5. Comparisons of the model results with the mathematical formulas in calculating MSD.

	MSD		
Point and coordinates	Formulas	Model	Difference[a]
Rectangles			
Point 1 (0,0), point 2 (600,0), point 3 (600,400), point 4 (0,400)	193.71	193.68	0.03
Point 1 (0,0), point 2 (360,0), point 3 (360,240), point 4 (0,240)	116.32	116.27	0.05
Point 1 (0,0), point 2 (160,0), point 3 (160,60), point 4 (0,60)	45.14	44.98	0.16
Scalene triangle			
Point 1 (0,0), point 2 (400,100), point 3 (300,400)	108.70	109.22	–0.52
Point 1 (0,0), point 2 (400,100), point 3 (100,400)	110.59	111.28	–0.69
Point 1 (0,0), point 2 (400,400), point 3 (100,400)	112.44	113.28	–0.84
Irregular shapes			
Point 1 (10,250), point 2 (40,330),point 3 (190,370), point 4 (360,350), point 5 (370,310), point 6 (330,100), point 7 (240,70), point 8 (150,70), point 9 (60,120)	111.42	112.73	–1.31
Point 1 (50,70), point 2 (10,190), point 3 (30,310), point 4 (90,360), point 5 (360,280), point 6 (370,200), point 7 (130,70)	104.36	105.47	–1.11
Point 1 (10,150), point 2 (10,290), point 3 (310,380), point 4 (380,340), point 5 (380,270), point 6 (240,110)	106.26	107.96	–1.70

[a]Formulas – model.

with the optimal landing location is also presented. Each progressively more shaded ring in the figures represents an increasing range of total harvesting costs. A landing located at any point within a given ring would incur the total harvesting costs associated with that ring. For example, if a landing is located anywhere in the first circle in Fig. 13*a*, the total cost to harvest the entire unit using the selected landing would range from US$45 917 to $50 000 or from $\$7.32/m^3$ to $\$7.97/m^3$.

Hypothetical harvest units

Cases 1–3 are used as the basis for the comparisons of the other factors, because they represent flat terrain, even volume distribution, and no obstacles of any kind. Figure 13 il-

Fig. 6. Three different hypothetical harvest units developed for the model applications.

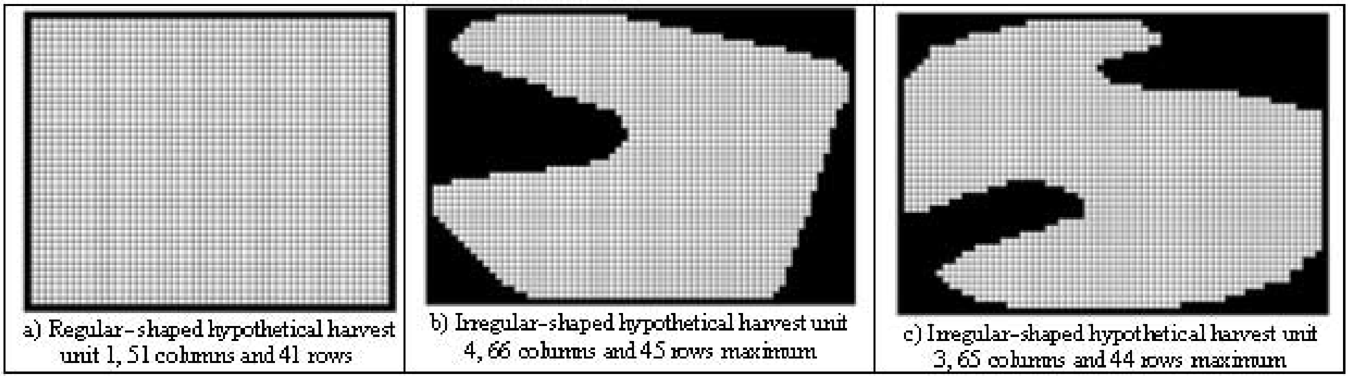

Fig. 7. DEM of harvest unit 1 with a maximum slope of (*a*) 20% for case 6, (*b*) 30% for case 7, and (*c*) 40% for case 8. The values at the bottom of the figure are elevations in metres.

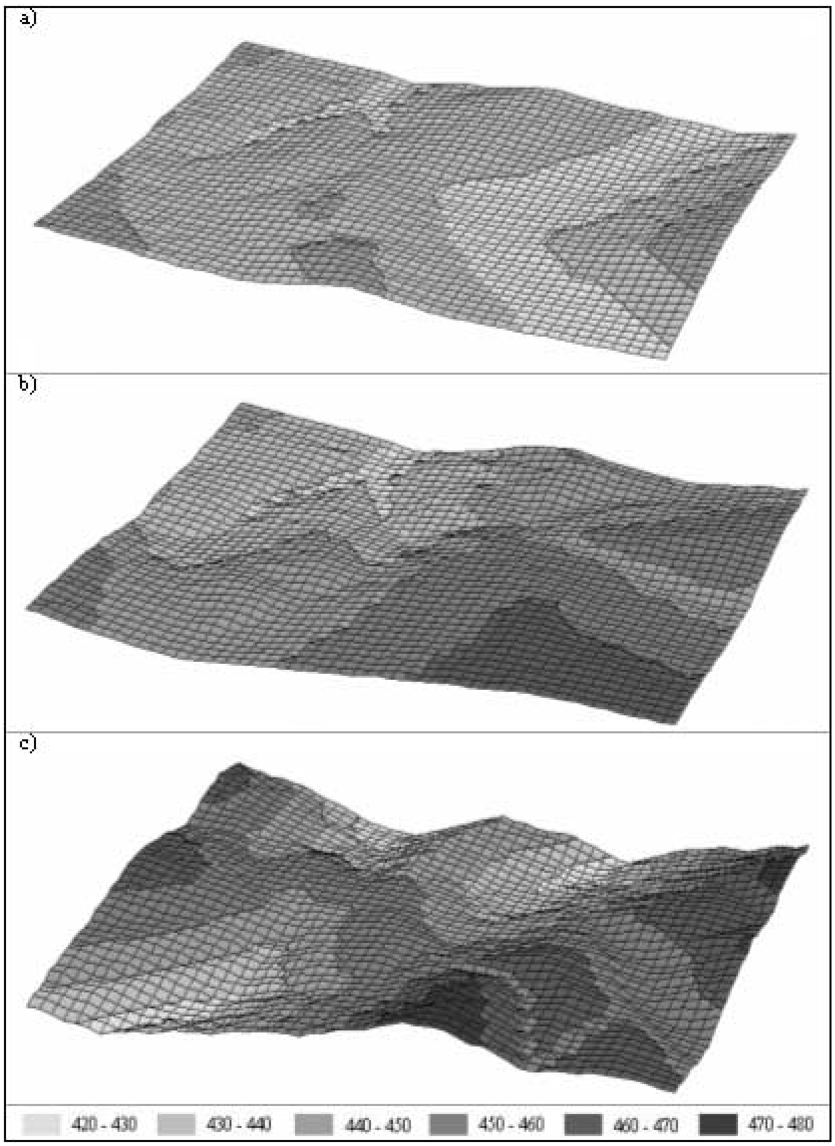

lustrates the results from these three cases. The concentric circles are perfectly symmetric in case 1, because skidding distances are straight lines (the shortest distances) between two points anywhere in the unit. The progressively darker shading of the rings around the optimal landing location show the skidding cost pattern, indicating that total skidding costs increase as the landing moves toward the harvest unit boundary. For the irregularly shaped boundaries (Fig. 13*b*

Fig. 8. DEM of harvest unit 1 with (*a*) one obstacle for case 9, (*b*) two obstacles for case 10, and (*c*) four obstacles for case 11. Circled areas are the steep areas, which skidders cannot pass through. The values at the bottom of the figure are elevations in metres.

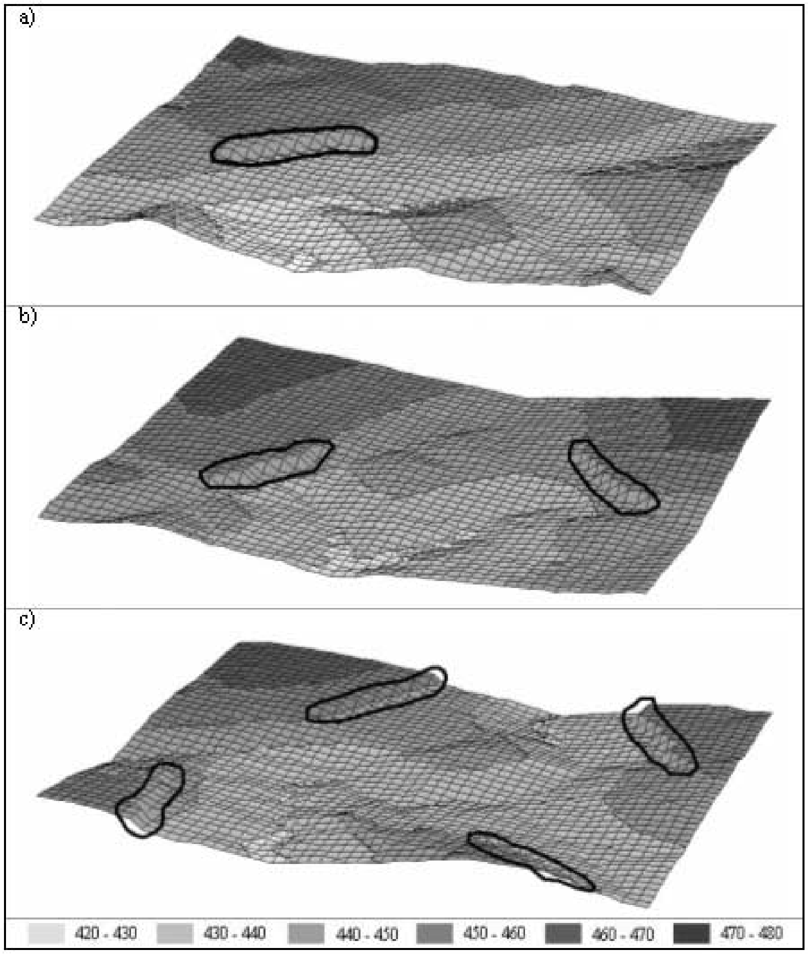

Fig. 9. (*a*) Case 12 with two different volume zones and (*b*) case 13 with three different volume zones.

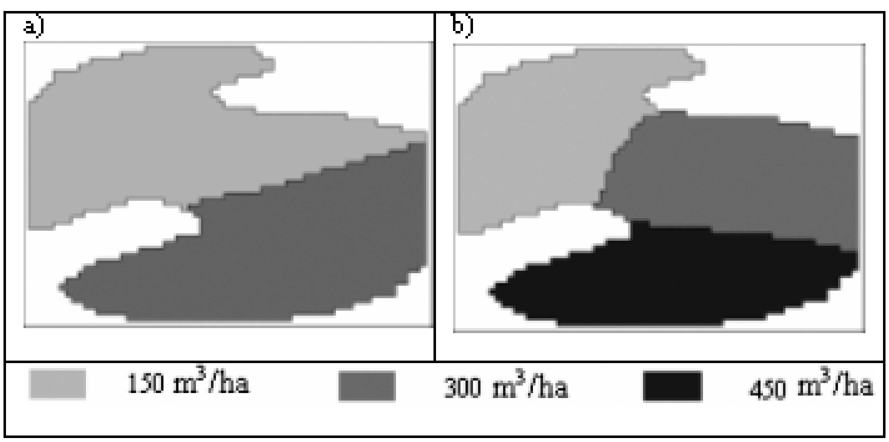

and 13*c*), the minimum TSCs increase and optimal landing locations are shifted compared with the regularly shaped unit (Fig. 13*a*), although all the units have the same area. This is because the geometric center of a harvest unit changes due to its irregular shaped boundary.

The results from cases 4 and 5, where obstacles caused by unit boundaries were considered, show that the total skidding costs increase faster than cases 2 and 3, respectively, as the landing moves toward the boundary (Fig. 14). This happens because skid trails have to follow the unit boundaries and if a landing is located close to the boundary, most skid trails become longer than straight lines. Interestingly, the presence of these obstacles in case 4 does not affect the optimal landing location but slightly increases the minimum TSCs (Fig. 14*a*). This is because the selected landing is not located near the boundary but is in the geometric centre of

Fig. 10. Harvest unit 1 developed for cases 14–16. The solid grid cell represents the takeoff point from an existing road. The values at the bottom of the figure are elevations in metres.

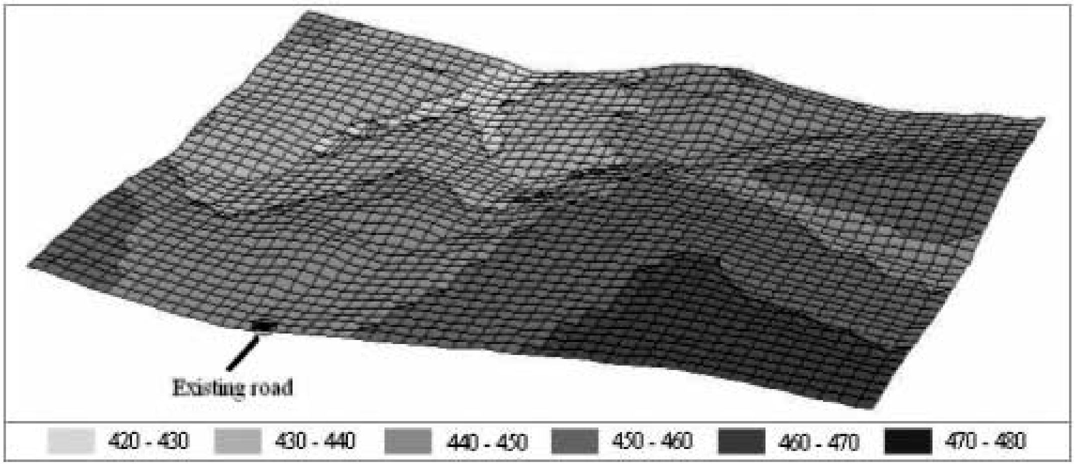

Table 6. Terrain and timber volume attributes of the 16 cases examined in this study.

	Hypothetical harvest unit (boundary shape)	Terrain steepness	Presence of obstacles	Timber volume distribution	Spur road construction
Case 1	Harvest unit 1 (regular)	Flat	No obstacles	Even	Not considered
Case 2	Harvest unit 2 (irregular)	Flat	No obstacles	Even	Not considered
Case 3	Harvest unit 3 (irregular)	Flat	No obstacles	Even	Not considered
Case 4	Harvest unit 2 (irregular)	Flat	One boundary obstacle	Even	Not considered
Case 5	Harvest unit 3 (irregular)	Flat	Two boundary obstacles	Even	Not considered
Case 6	Harvest unit 1 (regular)	20% maximum slope inclination	No obstacles	Even	Not considered
Case 7	Harvest unit 1 (regular)	30% maximum slope inclination	No obstacles	Even	Not considered
Case 8	Harvest unit 1 (regular)	40% maximum slope inclination	No obstacles	Even	Not considered
Case 9	Harvest unit 1 (regular)	30% maximum slope inclination	One obstacle	Even	Not considered
Case 10	Harvest unit 1 (regular)	30% maximum slope inclination	Two obstacles	Even	Not considered
Case 11	Harvest unit 1 (regular)	30% maximum slope inclination	Four obstacles	Even	Not considered
Case 12	Harvest unit 3 (irregular)	Flat	No obstacles	Two volume zones	Not considered
Case 13	Harvest unit 3 (irregular)	Flat	No obstacles	Three volume zones	Not considered
Case 14	Harvest unit 1 (regular)	30% maximum slope inclination	No obstacles	Even	US$10/m
Case 15	Harvest unit 1 (regular)	30% maximum slope inclination	No obstacles	Even	US$20/m
Case 16	Harvest unit 1 (regular)	30% maximum slope inclination	No obstacles	Even	US$30/m

the unit from which most areas can be still accessed through straight lines. However, case 5 has an irregular boundary that is large enough to affect the optimal landing location. The geometric centre does not serve as the least cost landing location any more, because large areas must be accessed from the centre through longer skidding distances. The model found the optimal landing location at row 27 and column 37, which is moved 50 m southeast (three rows down and four columns to the right). The minimum TSC increases by US$1715 compared with case 3 (Fig. 14*b*).

Fig. 11. The 10 m × 10 m DEM of an actual harvest unit located in the Mica Creek watershed, Idaho. The values at the bottom of the figure represent elevations in metres.

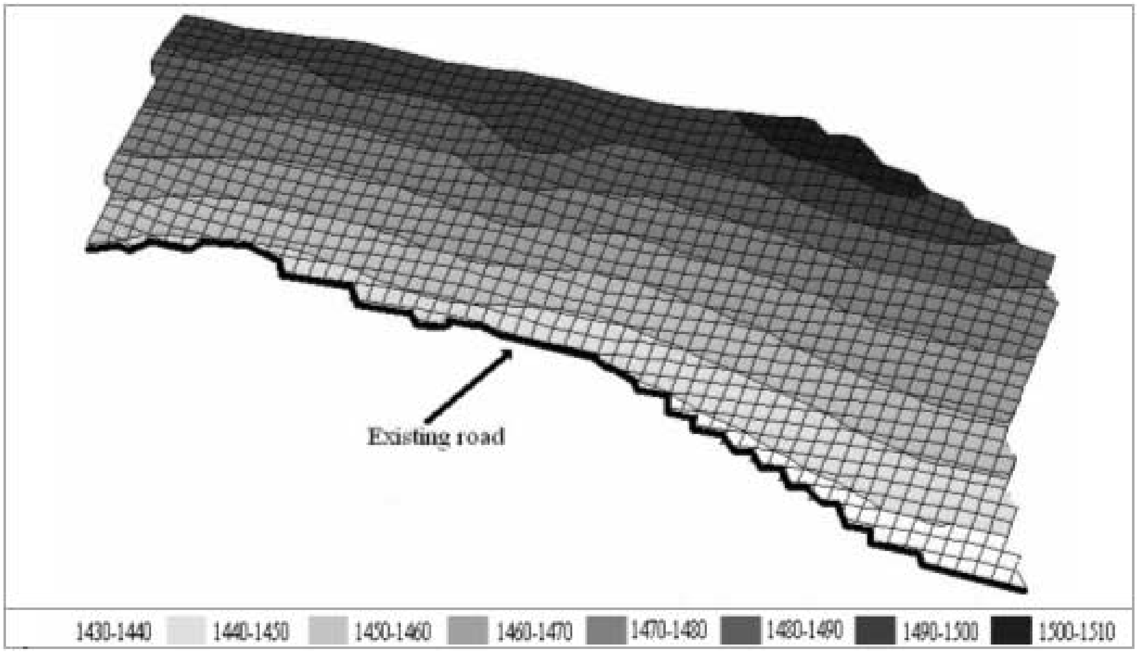

Fig. 12. Obstacles presented by ground slopes that are greater than 40%.

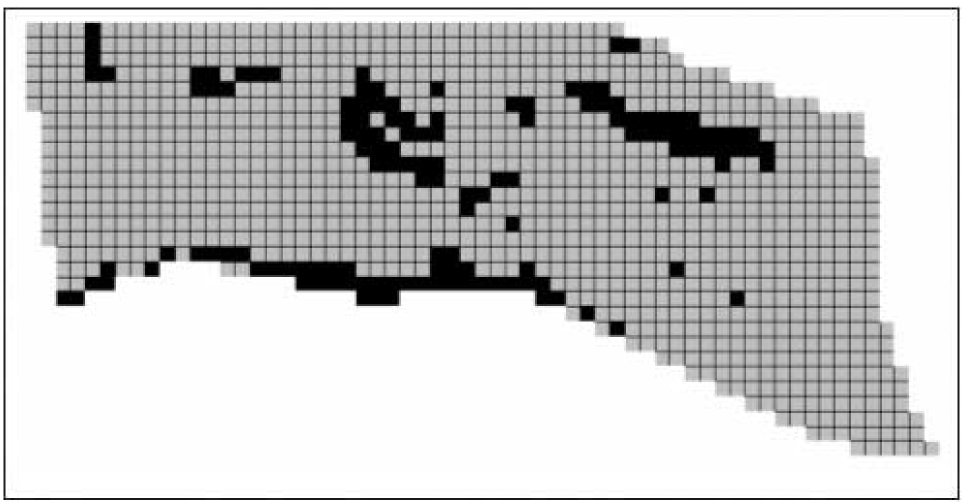

Figure 15 illustrates the model results from cases 6–8, where different terrain slopes are considered. The skidding cycle time equations used in this analysis estimate uphill skidding cycle time higher than downhill. As the results, landing locations are shifted to lower elevation areas in all three cases. Elevations at three landing locations in cases 6, 7, and 8 are 427 m, 434 m, and 445 m, respectively, whereas elevations at the centre of each unit are 431 m, 446 m, and 447 m, respectively, which would have been optimal landing locations if terrain slopes had not been considered. The minimum TSC is increased by US$1685, $2231, and $2870 in cases 6, 7, and 8, respectively, compared with case 1. This is because the skidding distance represented by a slope distance in the model increases as the terrain gets steeper.

The results from the computer model for cases 9–11 are presented in Fig. 16. These cases include the presence of obstacles caused by small steep areas that skidders cannot pass through. The results show that the optimal landing location is affected by the presence of those obstacles. For case 9 (with one obstacle), the optimal landing location is moved 10 m south (one row down; Fig. 16*a*) compared with case 1. For case 10 (with two obstacles), the landing is moved 10 m north (one row up, Fig. 16*b*), and for case 11 (with three obstacles), the landing is moved 14 m southeast (Fig. 16*c*). The minimum TSCs also increase in the three cases by US$1573, $1727, and $2686, respectively, compared with case 1. The skidding cost pattern differs significantly when more obstacles are considered. The deformed concentric circles in Fig. 16 show how quickly the skidding cost increases if the landing is located close to the places where skidding along a straight line is not feasible.

Fig. 13. Model results for (*a*) case 1, (*b*) case 2, and (*c*) case 3. The single solid cell shows the optimal landing location. Shaded rings show the different skidding cost ranges in dollars.

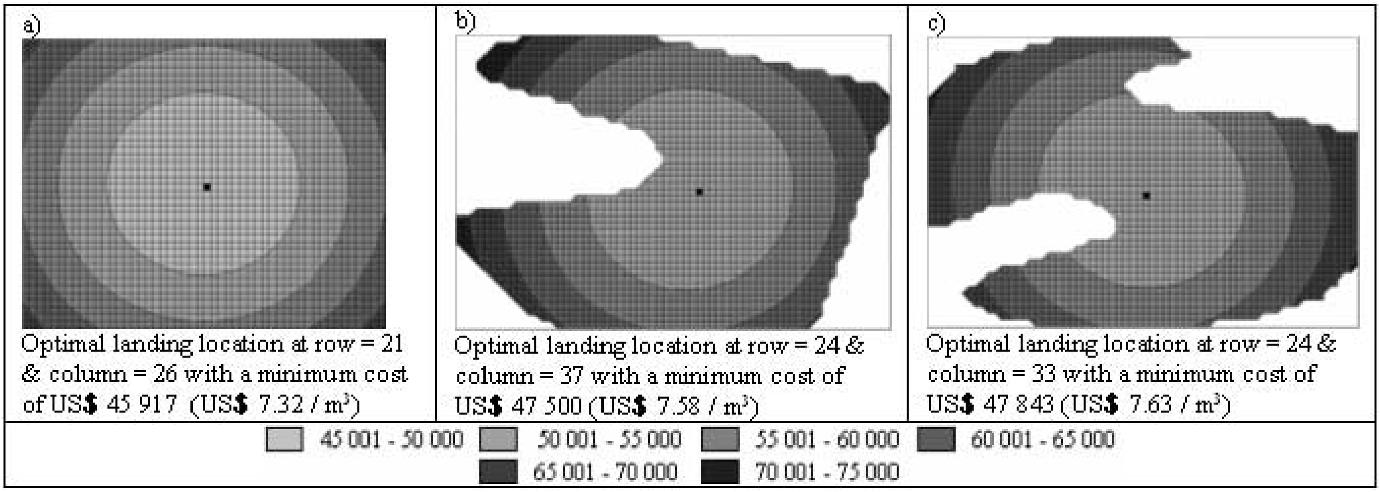

Fig. 14. Model results for (*a*) case 4 and (*b*) case 5. The single solid cell shows the optimal landing location. Shaded rings show the different skidding cost ranges in dollars.

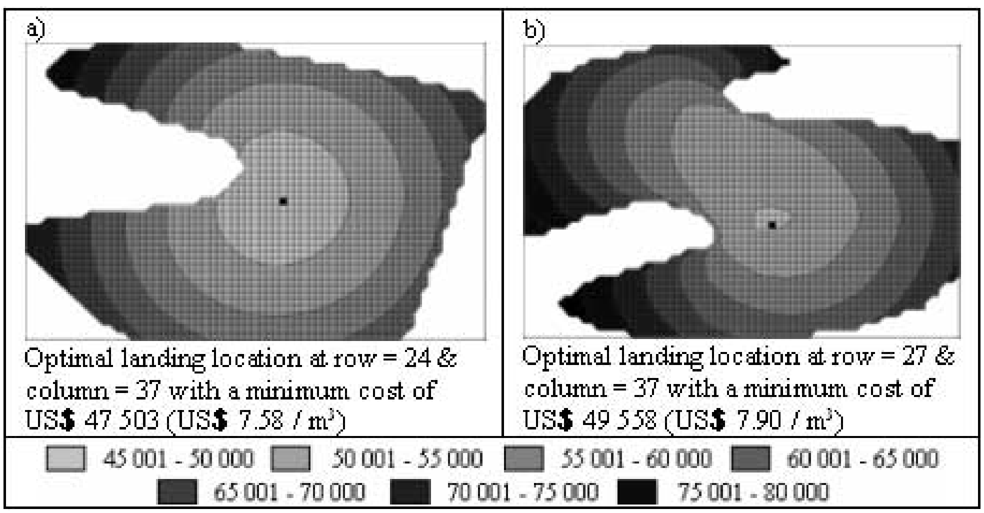

Figure 17 shows the results from cases 12 and 13, where different timber volume distribution is considered. In cases 12 and 13, the optimal landing locations as well as concentric circles are moved towards the area with higher volume density (Fig. 17*a* and 17*b*). As the results, the optimal landing location is moved 40 m south (four rows down) and 64 m southeast (five rows down and four columns to the right) in cases 12 and 13, respectively. The shift of landing location in cases 12 and 13 causes TSC per unit volume to decrease by US\$0.13/m^3 and \$0.28/m^3, respectively. The result indicates that we can benefit from shifting landing locations toward more volume areas and that volume distribution is an important factor in forest operations planning.

The model results from cases 14–16 are presented in Figs. 18 and 19 where different spur road costs (TRC) are considered. Figure 18 illustrates the spur road cost pattern for costs of US\$10/m, \$20/m, and \$30/m (Fig. 18*a*, 18*b*, and 18*c*, respectively), which shows how the TRC increases as the landing is located away from the exit point (row 41 and column 15). For example, if a landing is located in the darkest area in Fig. 18*a*, the cost of building a spur road to connect the existing road to the landing would be higher than US\$10 000.

Figure 19 shows the THC pattern from cases 14, 15, and 16 (Fig. 19*a*, 19*b* and 19*c*, respectively), which are calculated by adding TSC (Fig. 13*a*) and TRC (Fig. 18*a*, 18*b* and 18*c*). Optimal landing location was found at row 25 and column 22 for the three different cases, with a minimum THC of US\$49 291, \$51 556, and \$53 821, respectively. The optimal landing location shifted 57 m southwest (four rows down and four columns left), towards the cell representing the exit point, compared with case 1, where spur road construction cost is not considered. Although the base spur road construction cost differs, the optimal landing location remains the same for cases 14–16. This is because TRC are relatively small compared with THC (5.3%, 9.4%, and 13.2% of THC for cases 14, 15, and 16, respectively) and the base road construction cost of US\$30/m is not large enough to shift the landing location towards the existing road. We also found that when the road construction cost is

Fig. 15. Model results for (*a*) case 6, (*b*) case 7, and (*c*) case 8. The single solid cell shows the optimal landing location. Shaded rings show the different skidding cost ranges in dollars.

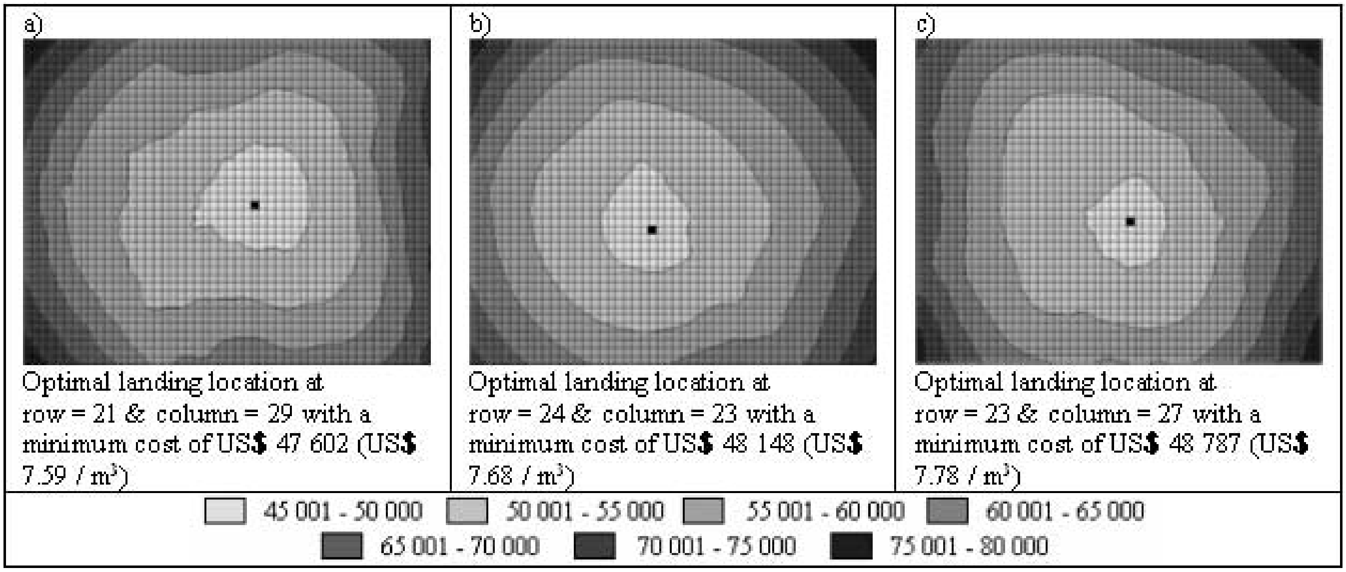

Fig. 16. Model results for (*a*) case 9, (*b*) case 10, and (*c*) case 11. The single solid cell shows the optimal landing location. Shaded rings show the different skidding cost ranges in dollars.

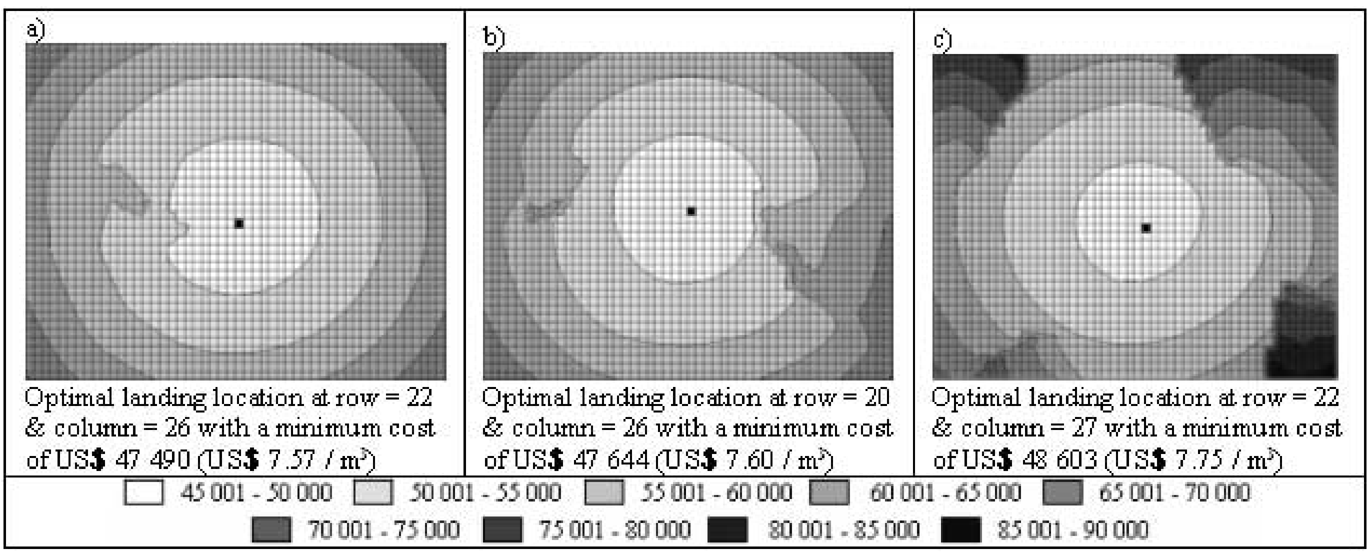

larger than US$33.1/m, the optimal landing location starts further shifting towards the existing road. The THC patterns resulted from cases 14–16 show that the more expensive TRC is, the quicker the harvesting cost increases as the landing is located away from the existing roads.

Actual harvest unit

When only TSC was considered, the optimal landing location was found at row 10 and column 33 with a minimum TSC of US$40 486 or $7.62/m^3 (Fig. 20). TRCs were estimated by the model using the base road construction cost of US$10 per horizontal metre (Fig. 21). Each progressively darker shaded band in Fig. 21 indicates a range of TRC when a landing is located in the band. Because existing roads are located at the bottom of the unit, the spur road construction cost increases as the landing is located away from the existing roads.

The model calculated the THC by adding the estimated spur TRC to the TSC for each candidate landing location (each grid cell in the harvest unit). Then, it selects the grid cell that has the minimum THC. This cell was found at row 19 and column 30 in the actual harvest unit (Fig. 22). The minimum THC associated with the optimal landing location is US$42 578 or $8.02/m^3. The optimal landing location is placed by the existing road to minimize the construction of a new spur road. This result indicates that the spur road cost exceeds the additional skidding cost caused by shifting the landing towards the existing roads. In fact, if the landing is located one row above, THC increases by US$635 because the increase of TRC (US$1136) exceeds the savings in TSC (US$501).

Fig. 17. Model results for (*a*) case 12 and (*b*) case 13. The single solid cell shows the optimal landing location. Shaded rings show the different skidding cost ranges in dollars.

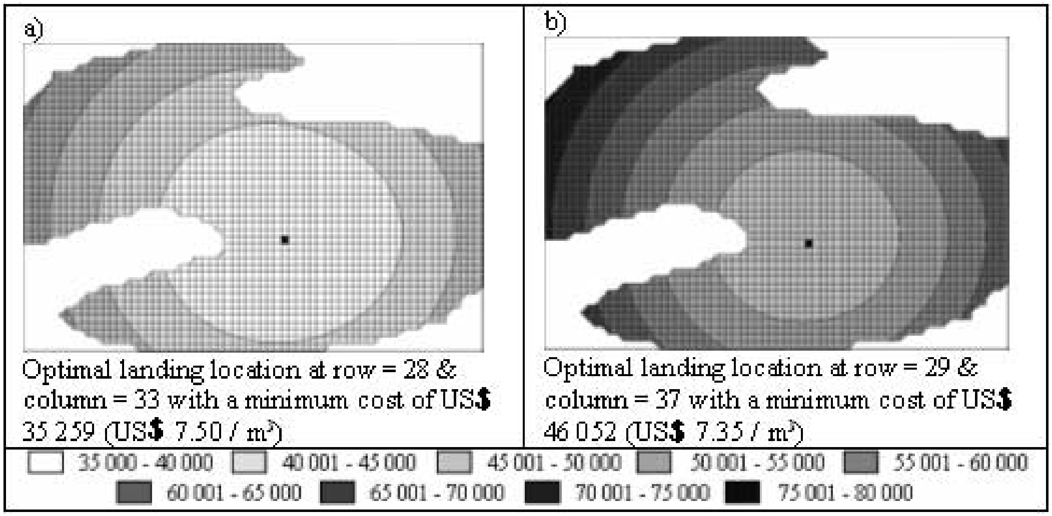

Fig. 18. Road construction cost of (*a*) US$10/m, (*b*) US$20/m, and (*c*) USD 30. The solid cell shows the existing road location. Shaded areas show the different skidding cost ranges in dollars.

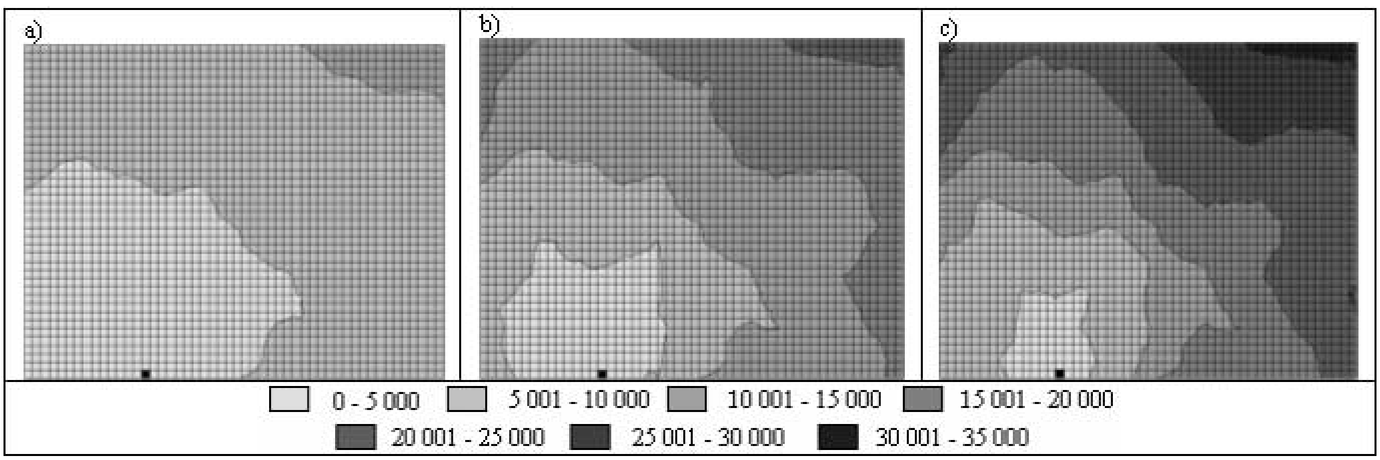

Fig. 19. Model results for (*a*) case 14, (*b*) case 15, and (*c*) case 16. The single solid cell indicates the optimal landing location. Shaded rings represent different skidding cost ranges in dollars. The solid path is the least cost spur road location.

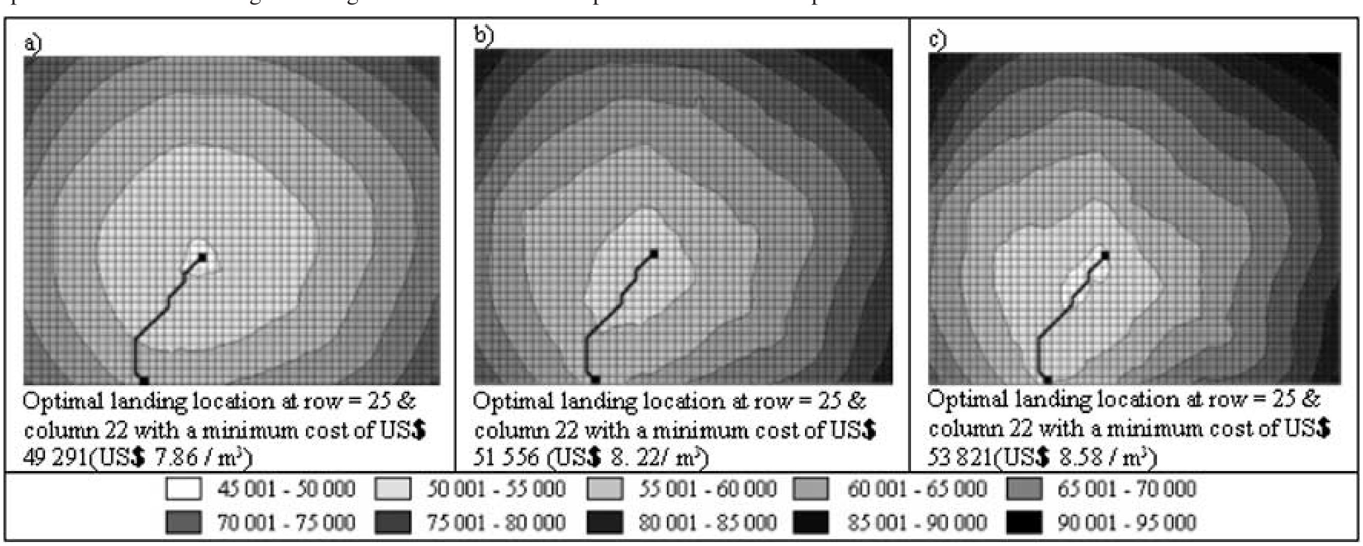

Fig. 20. Skidding cost patterns depending on the landing location in the actual harvest unit. Shaded areas represent different skidding cost ranges in dollars.

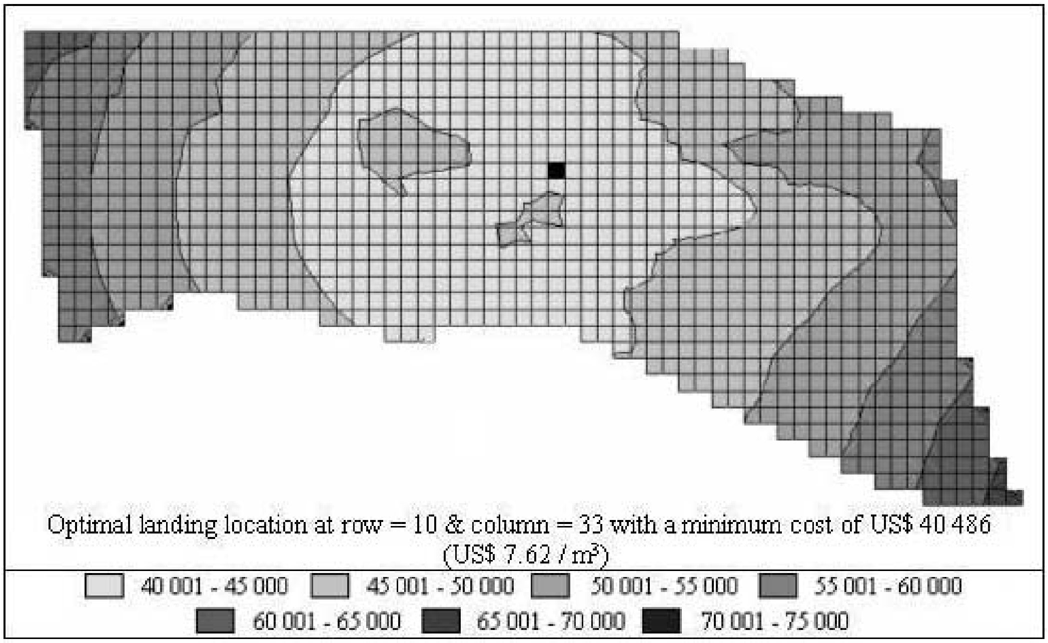

Fig. 21. Spur road construction cost patterns depending on the landing location in the actual harvest unit.

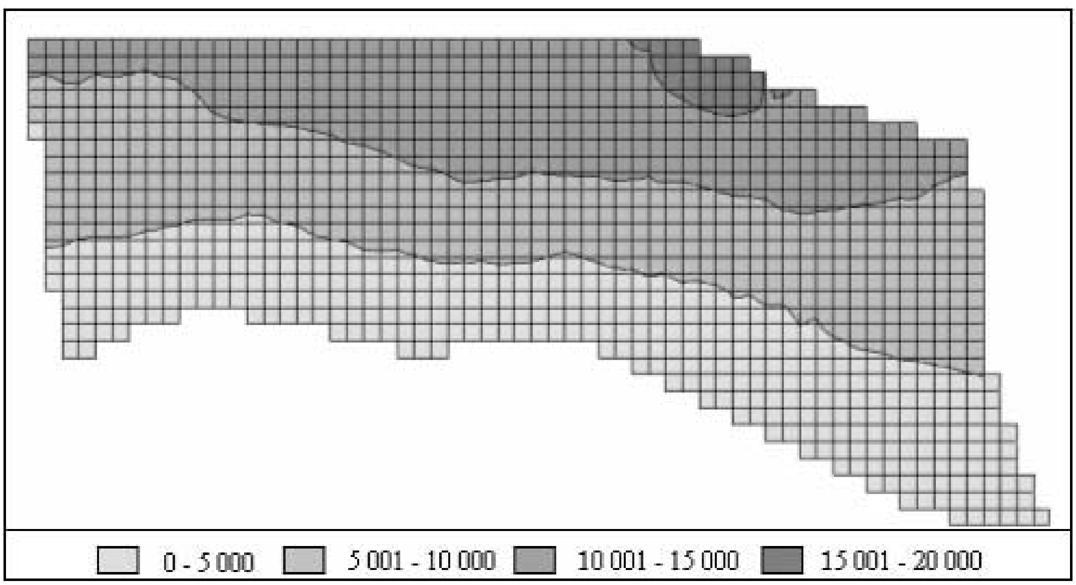

Summary of results

The results generated by the computer model for the 16 different cases and the one actual harvest unit show how the optimal landing location is affected by its influencing design factors. Terrain slopes represented by the maximum slope inclination of the harvest unit cause the optimal landing location to shift toward lower elevation areas mainly due to the cost function used in the analysis, which penalizes uphill skidding over downhill. Irregular harvest unit boundaries show a marginal effect on optimal landing locations for the cases analyzed. However, when the harvest unit boundary becomes an obstacle, it redirects skid trails, and the landing location changes depending on the irregularity of the boundary. Different volume distributions have relatively large effects on landing locations. The presence of steep areas marginally affects landing locations compared with the base case, but it dramatically changes skidding cost patterns. Lastly, the consideration of road cost largely affects the optimal landing location, but the different levels of road costs analyzed were not large enough to change the optimal landing location.

The effects of landing location changes caused by these design factors are measured in terms of cost savings (Table 7). Landing locations in each case are presented in terms of grid cell addresses (rows and columns) with estimated THCs in the “Considering the factor” column in Ta-

Fig. 22. Model results of total harvesting cost for case study. The single solid cell indicates the optimal landing location. Shaded areas represent different skidding cost ranges in dollars.

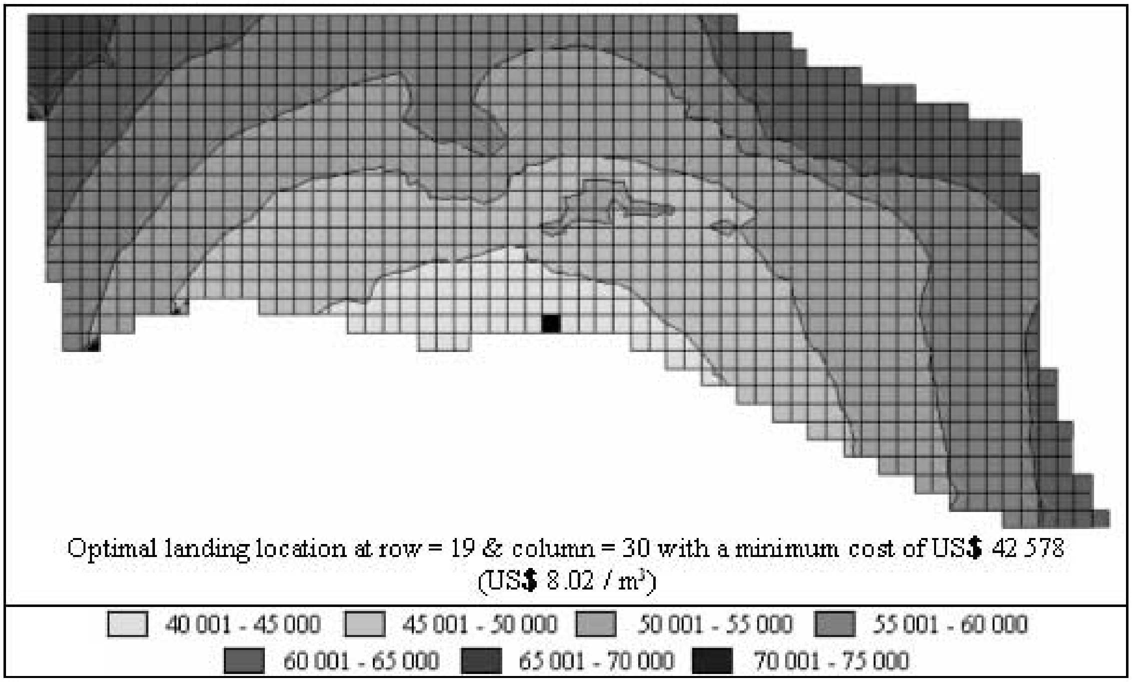

Table 7. Estimated cost savings made by considering each of design factors in the planning.

Factor and case	Considering the factor: Row, column	Considering the factor: Cost (US$)	Without considering the factor: Row, column	Without considering the factor: Cost (US$)	Cost savings (US$)
Boundary					
4	24, 37	47 503	24, 37	47 503	0 (0.0)
5	27, 37	49 558	24, 33	50 869	1311 (2.6)
Terrain					
6	21, 29	47 602	21, 26	48 405	803 (1.7)
7	24, 23	48 148	21, 26	49 476	1328 (2.7)
8	23, 27	48 787	21, 26	48 974	187 (0.4)
Obstacle					
9	22, 26	47 490	21, 26	47 501	11 (0.0)
10	20, 26	47 644	21, 26	47 676	32 (0.1)
11	22, 27	48 603	21, 26	48 629	26 (0.1)
Volume					
12	28, 33	35 259	24, 33	35 856	597 (1.7)
13	29, 37	46 052	24, 33	47 077	1025 (2.2)
Roads					
14	22, 25	49 291	21, 26	51 772	2481 (4.8)
15	22, 25	51 556	21, 26	57 196	5640 (9.9)
16	22, 25	53 821	21, 26	63 264	9443 (14.9)

ble 7. Each case is then compared with its corresponding base case which provides the optimal landing location without considering the specific design factor. This landing location is presented in Table 7 in the "Without considering the factor" column. The THC associated with this base case landing location is estimated under the circumstance where the design factor affects harvesting costs, which is shown in the cost column under "Without considering the factor". We present this cost difference between the two landing locations as a cost saving made by considering specific design factors in the planning. For example, case 7 represents the case where terrain slopes and skidding directions (uphill and downhill) are considered in the planning. As a result, the landing location is shifted to row 24 and column 23 from row 21 and column 26, which would have been the landing location without considering terrain slopes. The THC for this base case landing location (row 21 and column 26) is then estimated under the circumstance where terrain slopes affect skidding costs, which is US$49 476. The difference between this cost and theTHC associated with the new landing location (US$48 148) is presented as a cost saving (US$1328) made by considering ground slopes in the planning. Compared with the corresponding base cases, most design factors except for the spur road construction provide marginal cost savings for the cases analyzed in this study.

Conclusions

A computerized model has been developed to determine the optimal landing location in a timber harvest unit. The real advantage of the model is that it can consider a wide range of physical and vegetation attributes of harvest units that may affect the optimal landing locations. Although the magnitude of the cost savings resulted from considering each design factor is relatively marginal in the cases analyzed in this study, our results show physical and vegetation attributes of a harvest unit can affect skidding and road cost patterns and, thus, need to be considered when a landing location is selected. The effects of individual design factors most likely vary case by case, and the results of this study should not be used to rank individual design factors in terms of the magnitude of their effects on the optimal landing location.

Individual harvest units have their unique physical and vegetation attributes, and therefore, locating landings should be approached as case-specific problems. Rules of thumbs and rough approximations may not provide enough information for finding the optimal landing locations. Although the applications of this model are limited to ground-based timber harvest units, analytical tools such as this model can help forest professionals make better decisions in forest operations planning by providing thorough analyses that consider various design factors for individual harvest units.

Even though the model uses a complete enumeration, a landing placement problem dealing with only one harvest unit is small enough to solve quickly. The model took less than 2.5 min for a Pentium 4 computer to analyze the most complicated case. The complete enumeration of all possible solutions ensures solution optimality that is not often afforded by other models. Our model results can be thus used for verification of other models.

Data required to run the model can be easily obtained. Advanced remote sensing (e.g., LIDAR) and GIS technologies have made it possible to collect accurate terrain and vegetation attributes. With the increasing availability of accurate and high-resolution spatial data, the computerized approaches such as this model will be more and more demanded for detailed forest operations planning.

The model should be further improved and developed to remove several assumptions made for the analysis. For example, the model assumes an integer number of skidding cycles per grid cell, which does not allow combining small timber volumes in adjacent grid cells. The model does not directly account for the ground slope effects on skidder cycle times. It is a well-known fact by practitioners that the slope of the skid trails and skidding directions have a significant impact on production, but very few cost models have been developed that distinctively account for uphill, downhill, and accurately estimate slope-dependent cycle times. Proper and accurate cost estimation models are necessary for better quality and reliable solutions of the model. The rough estimate of road construction costs is another limitation to be improved. Lastly, the further development should include the expansion of the model capability to consider designated skid trails, multiple log landings in one harvest unit, contiguous landing along existing roads, different harvesting methods, or the combinations of these options.

References

Anderson, A., and Nelson, J. 2004. Projecting vector-based road networks with a shortest path algorithm. Can. J. For. Res. **34**: 1444–1457. doi:10.1139/x04-030.

Bradner, M., Klobucher, F., Girard, J., and Fullaway, S. 1933. An analysis of log production in the ‘inland empire’ region. USDA For. Serv. Tech. Bull. No. 355.

Brandstrom, A. 1933. Analysis of logging costs and operating methods in the Dauglas-fir region. Charles Lathrop Pack Forestry Foundation, Seattle, Wash.

Chung, W., Sessions, J., and Heinimann, H. 2004. An application of heuristic network algorithm to cable logging layout design. Int. J. For. Eng. **15**: 11–24.

Clarke, K. 2003, Getting started with geographic information systems. 4th ed. Prentice Hall, Upper Saddle River, N.J.

Dijkstra, E. 1959. A note on two problems in connexion [sic.] with graphs. Numerische Math. 1: 269–271.

Donnelly, D. 1978. Computing average skidding distance for logging areas with irregular boundaries and variable log density. USDA. For. Serv.Gen. Tech. Rep. RM-58.

Greulich, F. 1989. The calculation of average yarding distance to a centralized landing, given a polygonal mesh approximation of the setting surface. Can. J. For. Res. **19**: 141–144.

Greulich, F. 1991. Optimal landing location on flat, uniform terrain. Can. J. For. Res. **21**: 573–584.

Greulich, F. 2003. Transportation networks in forest harvesting: early development of the theory. *In* Proceedings of S3.04/3.06/3.07 Subject Area, IUFRO International Seminar on New Roles of Plantation Forestry Requiring Appropriate Tending and Harvesting Operations, 2–5October 2002, Tokyo, Japan. IUFRO, Vienna.

Han, H.-S., and Renzie, C. 2005. Productivity and cost of partial harvesting method to control mountain pine beetle infestations in British Columbia. West. J. Appl. For. **20**: 128–133.

Liu, S., and Corcoran, T. 1993. Road and landing spacing under the consideration of surface dimensions of roads and landings. Int. J. For. Eng. **5**: 49–53.

Love, R. 1972. A computational procedure for optimally location a facility with respect to several rectangular regions. J. Reg. Sci. **12**: 233–242.

Matthews, D. 1942. Cost control in the logging industry. McGraw-Hill Book, New York.

Perkins, R., and Lynn, K. 1979. Determining average skidding distance on rough terrain. J. For. **77**: 84–88.

Peters, P. 1978. Spacing of roads and landings to minimize timber harvest cost. For. Sci. **24**: 209–217.

Peters, P., and Burke, J. 1972. Average skidding distance on irregular shaped timber harvest settings. USDA. For. Serv. Pac. Northwest Res. Stn. Res. Note PNW-178.

Roberts, F. 1984. Applied combinatorics. Prentice-Hall, Inc., Englewood Cliffs, N.J.

Segebaden von, G. 1964. Studies of cross-country transport distances and road net extension. Stud. For. Sued. No. 18.

Suddarth, S., and Herrick, A. 1964. Average skidding distance for theoretical analysis of logging costs. Purdue Univ. Agric. Exp. Stn. Res. Bull. **789**

Tan, J. 1999. Locating forest roads by a spatial and heuristic procedure using microcomputers. Int. J. For. Eng. **10**: 91–100.

Thompson, M. 1992. Considering overhead costs in road and landing spacing models. Int. J. For. Eng. **3**: 13–19.

Tucek, J. 1999. Algorithms for skidding distance modeling on a raster digital terrain model. Int. J. For. Eng. **10**: 67–79.